Heart Vessels (2013) 28:646–657
DOI 10.1007/s00380-012-0311-0

ORIGINAL ARTICLE

Atrial natriuretic peptide exerts protective action against angiotensin II-induced cardiac remodeling by attenuating inflammation via endothelin-1/endothelin receptor A cascade

Shuichi Fujita · Naoshi Shimojo · Fumio Terasaki · Kaoru Otsuka · Noriko Hosotani · Yuka Kohda · Takao Tanaka · Tomohiro Nishioka · Toshimichi Yoshida · Michiaki Hiroe · Yasushi Kitaura · Nobukazu Ishizaka · Kyoko Imanaka-Yoshida

Received: 29 June 2012 / Accepted: 30 November 2012 / Published online: 1 January 2013

Abstract We aimed to investigate whether atrial natriuretic peptide (ANP) attenuates angiotensin II (Ang II)-induced myocardial remodeling and to clarify the possible molecular mechanisms involved. Thirty-five 8-week-old male Wistar–Kyoto rats were divided into control, Ang II, Ang II + ANP, and ANP groups. The Ang II and Ang II + ANP rats received 1 μg/kg/min Ang II for 14 days. The Ang II + ANP and ANP rats also received 0.1 μg/kg/min ANP intravenously. The Ang II and Ang II + ANP rats showed comparable blood pressure. Left ventricular fractional shortening and ejection fraction were lower in the Ang II rats than in controls; these indices were higher ($P < 0.001$) in the Ang II + ANP rats than in the Ang II rats. In the Ang II rats, the peak velocity of mitral early inflow and its ratio to atrial contraction-related peak flow velocity were lower, and the deceleration time of mitral early inflow was significantly prolonged; these changes were decreased by ANP. Percent fibrosis was higher ($P < 0.001$) and average myocyte diameters greater ($P < 0.01$) in the Ang II rats than in controls. ANP decreased both myocardial fibrosis ($P < 0.01$) and myocyte hypertrophy ($P < 0.01$). Macrophage infiltration, expression of mRNA levels of collagen types I and III, monocyte chemotactic protein-1, and a profibrotic/proinflammatory molecule, tenascin-C (TN-C) were increased in the Ang II rats; ANP significantly decreased these changes. In vitro, Ang II increased expression of TN-C and endothelin-1 (ET-1) in cardiac fibroblasts, which were reduced by ANP. ET-1 upregulated TN-C expression via endothelin type A receptor. These results suggest that ANP may protect the heart from Ang II-induced remodeling by attenuating inflammation, at least partly through endothelin 1/endothelin receptor A cascade.

Keywords ANP · Cardiac remodeling · Tenascin-C · Inflammation · Endothelin-1

S. Fujita · N. Shimojo · F. Terasaki · K. Otsuka · Y. Kitaura · N. Ishizaka (✉)
Department of Cardiology, Osaka Medical College, 2-7 Daigaku-machi, Takatsuki, Osaka 569-8686, Japan
e-mail: ishizaka@poh.osaka-med.ac.jp

N. Shimojo · T. Nishioka · T. Yoshida · K. Imanaka-Yoshida (✉)
Department of Pathology and Matrix Biology, Mie University Graduate School of Medicine, 2-174 Edobashi, Tsu, Mie 514-8507, Japan
e-mail: kyimanaka@gmail.com

N. Shimojo · T. Yoshida · K. Imanaka-Yoshida
Mie University Research Center for Matrix Biology, 2-174 Edobashi, Tsu, Mie 514-8507, Japan

N. Hosotani · Y. Kohda
Laboratory of Pharmacotherapy, Osaka University of Pharmaceutical Sciences, 4-20-1 Nasahara, Takatsuki, Osaka 569-1094, Japan

T. Tanaka
Department of Nursing Science, Baika Women's University, 2-19-5 Shukunosho, Ibaraki, Osaka 567-8578, Japan

M. Hiroe
Department of Cardiology, National Center of Global Health and Medicine, 1-2-1Toyama, Shinjuku-ku, Tokyo 162-8655, Japan

Introduction

Atrial natriuretic peptide (ANP) was originally identified as a diuretic/natriuretic and vasodilating hormone released by the heart in response to myocardial stretch and overload. Recent reports have demonstrated that ANP exerts various beneficial effects on the heart [1–3], For example. ANP

suppresses the renin-angiotensin-aldosterone system (RAAS), endothelin synthesis, and sympathetic nerve activity [4], whereas it enhances adiponectin production and regulates cell growth and apoptosis (reviewed in [5, 6]), as a circulating hormone as well as a local autocrine and/or paracrine factor. Indeed, ANP exhibits therapeutic efficacy against chronic heart failure [7–9], acute heart failure [10–13], and acute myocardial infarction [14–17] in humans as well as rat models of acute myocardial infarction–reperfusion [18] and autoimmune myocarditis [19]. However, the detailed molecular mechanisms of these cardioprotective functions remain uncertain.

Left ventricular (LV) remodeling is an important factor related to the prognosis of heart disease. Histological features of LV remodeling include interstitial fibrosis and myocyte hypertrophy. Enhanced myocardial stiffness caused by increased interstitial fibrosis is known to lead to diastolic heart failure. Recently, increasing attention has been paid to the fact that RAAS overactivation-mediated inflammation plays a significant role in the development of cardiac fibrosis during ventricular remodeling [20–23]. Fibrotic lesions are formed via a multistep process of synthesis and degradation of various extracellular matrix molecules, including tenascin-C (TN-C). TN-C is an extracellular glycoprotein that is weakly expressed in healthy adult hearts, but it is transiently upregulated in association with tissue injury and inflammation [24–30]. This specific expression pattern makes TN-C a valuable marker for inflammatory disease activity [25, 27]. Using a mouse model, we previously reported that TN-C may be involved in the progression of hypertensive myocardial fibrosis and that elevated TN-C expression may be a marker for active progression of fibrosis in the heart [28]. Furthermore, TN-C has diverse biological functions and is considered to be a key molecule during the progression of inflammation and fibrosis (reviewed in [31, 32]). We investigated whether ANP attenuates cardiac fibrosis in a rat model of Ang II-induced ventricular remodeling and the molecular mechanism involved, especially focusing on TN-C. Cardiac function, histological changes, and expression of molecules related to fibrosis and inflammation, which include collagen type I, collagen type III, TN-C, monocyte chemotactic protein-1 (MCP-1), and endothelin-1 (ET-1) were examined in the heart of model rats treated with Ang II with or without ANP. Furthermore, the direct effects of ANP on TN-C synthesis and the signaling pathways involved were studied in cultured cardiac fibroblasts.

Materials and methods

Animal experiments were performed in accordance with the *Guide for the Care and Use of Laboratory Animals* published by the US National Institutes of Health (publication no. 85-23, revised 1996), and the study was approved by our Institutional Animal Research Committee. Experiments were performed on 8-week-old male Wistar–Kyoto rats that weighed 250–280 g before study initiation. The rats were fed a standard rat-chow diet and had free access to tap water. Thirty-five rats were randomly divided into four treatment groups (control, $n = 10$; Ang II, $n = 10$; Ang II + ANP, $n = 10$, ANP, $n = 5$). All rats were anesthetized with 3 % isoflurane on a volume-cycled ventilator (Univentor; Bio Research Center, Nagoya, Japan) for small animals. In Ang II and Ang II + ANP groups, a midline incision was made in the lumbar region for insertion of osmotic mini-pumps (model 2002; ALZET, Palo Alto, CA, USA; mean filling volume, 0.234 ml) filled with Ang II (Peptide Institute, Osaka, Japan), which was infused at 1 μg/kg/min for 14 days. The dose used in this study was determined on the basis of preliminary experiments. For the administration of saline or ANP, control, Ang II + ANP, and ANP groups bearing the mini-pump were fitted with a fluid-delivery infusion pump (10 ml Infu-disk; MED-e-CELL, San Diego, CA, USA) attached to the back. These external infusion pumps were filled with saline or carperitide, a recombinant α-human ANP (Daiichi-Sankyo Pharmaceutical, NY, USA), dissolved in distilled water and released at 0.1 μg/kg/min for 14 days. The pump was connected to the right or left jugular vein by a small polyethylene catheter. The rats were weighed on days 0, 3, 6, 10, and 14, and systolic blood pressure and heart rate were measured using a tail-cuff method without anesthesia on the same days. On day 14, the rats were deeply anesthetized with isoflurane and euthanized. The hearts were dissected and weighed, and a part of the ventricle was separated from the heart, frozen in RNAlater (Ambion, Huntington, UK), and stored at −80 °C until use.

Echocardiographic measures of cardiac function

LV function was assessed using a two-dimensional guided M-mode ultrasound system (VIVID7; GE Medical Systems, Tokyo, Japan). Images of the short-axis view of the left ventricle at the level of the papillary muscle were recorded to assess cardiac function. The end-diastolic LV dimension (LVDd) and end-systolic LV dimension (LVDs) were measured directly by echocardiography. The LV fractional shortening (FS) and LV ejection fraction (EF) were calculated as percentages from the LVDd and LVDs values. The LV diastolic function was evaluated by recording the pulse-wave Doppler spectra of transmitral flow. The peak velocity of mitral early inflow (*E*), its ratio to atrial contraction-related flow peak velocity (*E*/*A*), and the deceleration time of mitral early inflow (DcT) were also

measured. Echocardiography was performed on the 14th day after study initiation in all rats.

Histological analysis

Histological analysis was performed on five hearts from each group. The left ventricle was removed, fixed in 4 % paraformaldehyde, and embedded in paraffin. Three-micrometer-thick sections were prepared and stained with hematoxylin–eosin for evaluation of myocyte hypertrophy and with Sirius Red for evaluation of myocardial fibrosis. To determine the average myocyte size, the shortest transverse diameter was measured in 50 transverse sections per heart (×200 magnification), which contained the cross section of a myocyte with its nucleus. To determine the percent area of myocardial interstitial and perivascular fibrosis, the Scion imaging system (Scion, Frederick, MD, USA) was used as described previously [28]. To evaluate TN-C expression and the number of macrophages in the myocardium, we performed immunohistochemistry as described previously [33]. In brief, a mouse monoclonal antibody for TN-C (4F10TT; IBL, Gunma, Japan; 1:100 dilution) and a mouse monoclonal antibody against the macrophage marker cluster of differentiation 68 (CD68; DAKO Japan, Tokyo, Japan; 1:100 dilution) were used. Immunoreactivity was evaluated using the avidin–biotin–peroxidase complex method (ScyTek Laboratories, Logan, UT, USA). The reactions were visualized using diaminobenzidine, and nuclei were counterstained with hematoxylin. Quantitative analysis of tissue macrophages was performed using the CD68 antibody stain. For each-specimen, three randomly selected photomicrographs (×400 magnification) of the anterior, lateral, and posterior ventricular walls, as well as the interventricular septum, were examined (12 fields/specimen). The numbers of CD68-positive cells were counted in each region and expressed as the number of inflammatory cells per unit area (1 mm^2).

Immunofluorescence double labeling was applied to colocalize TN-C, and either α-smooth muscle actin (SMA)-positive cells or macrophages. Anti-α-SMA mouse monoclonal primary antibodies (Thermo Fisher Scientific, Yokohama, Japan; 1:100 dilution) were used for the detection of α-SMA-positive cells, and anti-CD68 mouse monoclonal primary antibodies (DAKO Japan; 1:100 dilution) were used for detection of macrophages. Biotinylated antimouse immunoglobulins (EPOS; Dako Japan; 1:250 dilution) were then used as part of the enhanced polymer one-step staining system, followed by incubation in streptavidin labeled with Alexa 448 (Molecular Probes, Eugene, OR, USA; 1:300 dilution). For detection of TN-C, anti-TN-C polyclonal rabbit antibody [33], and goat anti-rabbit immunoglobulins labeled with Alexa 555 (Molecular Probes; 1:300 dilution) were used. Fluoromount (Diagnostic BioSystem, Pleasanton, CA, USA) was used to mount stained sections on coverslips. Laser scanning confocal fluorescence microscopy combined with differential interference contrast imaging was performed using LSM 510 META Ver. 3.2 (Zeiss, Göttingen, Germany). Brightness and contrast adjustments along with necessary cropping were performed using Photoshop Elements 8.0 (Adobe, San José, CA, USA).

Real-time reverse transcription–polymerase chain reaction (real-time RT-PCR)

Total RNA was isolated from five hearts from each group and real-time RT-PCR performed to measure the mRNA expression levels of collagen type I, collagen type III, TN-C, MCP-1, ET-1, and glyceraldehyde-3-phosphate dehydrogenase (GAPDH). Quantitative PCR was performed using a Light Cycler (LightCycler FastStart DNA Master PLUS SYBR Green I; Roche Diagnostics; Mannheim, Germany). Amplification specificity was checked using a melting curve according to the manufacturer's instructions. The mRNA expression of each target was normalized to that of GAPDH. The forward and reverse primers are listed in Table 1.

Cell cultures

Cardiac fibroblasts were obtained from the ventricles of Wistar–Kyoto rats and grown in Iscove's modified

Table 1 Oligonucleotide primers used for real-time RT-PCR

Gene	Primers
Collagen type I	
Forward	5′-GCT TGG ATG GCT GCA C-3′
Reverse	5′-GGT GGG AGG GAA CCA GAT T-3′
Collagen type III	
Forward	5′-GGA AAA GAT GGA TCA AGT GGA C-3′
Reverse	5′-CTG GCT GTC CAG GGT GAC-3′
MCP-1	
Forward	5′-ATG CAG GTC TCT GTC ACG-3′
Reverse	5′-CAT TGG GAT CAT CTT GCC-3′
TN-C	
Forward	5′-ACC AAC TGT GCC CTG TCC TA-3′
Reverse	5′-GAT TTC GGA AGT TGC TGG GT-3′
ET-1	
Forward	5′-AGC TGG GAA AGA AGT GTA TC-3′
Reverse	5′-TCT GTA GAG TTC CGC TTT CA-3′
GAPDH	
Forward	5′-TAC ACT GAG GAC CAG GTT G-3′
Reverse	5′-CCC TGT TGC TGT AGC CAT A-3′

Dulbecco's medium (IMDM) supplemented with 10 % fetal bovine serum as described previously [34]. The experiments were performed on secondary cultures. Cells were plated in Multiwell 6-well plates (Becton–Dickinson, Franklin Lakes, NJ, USA) at 3×10^5 cells/well for 48 h in serum-free IMDM, and then treated with ET-1 (3×10^{-9}, 1×10^{-8}, 3×10^{-8}, and 1×10^{-7} mol/l) or Ang II (1×10^{-9} mol/l) for 6 h. To determine whether ET-1 is involved in the upregulation of Ang II-induced (1×10^{-9} mol/l) TN-C mRNA expression, the endothelin receptor (ET-R) antagonist bosentan (1×10^{-6} or 1×10^{-5} mol/l) was also used. To clarify the signaling pathways induced by Ang II, we coapplied the selective endothelin A receptor (ET-RA) antagonist BQ 123 (1×10^{-7}, 3×10^{-7}, and 1×10^{-6} mol/l) and/or the selective endothelin B receptor (ET-RB) antagonist BQ 788 (1×10^{-7}, 3×10^{-7}, and 1×10^{-6} mol/l). To examine if ANP blocks Ang II-induced TN-C expression, the cells were pretreated with ANP (1×10^{-8} or 1×10^{-7} mol/l) for 6 h and then stimulated with Ang II (1×10^{-9} mol/l) for 6 h. Total RNA was isolated from the treated cells using ISOGEN (Nippon Gene, Toyama, Japan), and the relative ET-1 or TN-C mRNA levels were determined by quantitative real-time RT-PCR.

Statistical analyses

All quantitative data are expressed as means ± standard deviation (SD). Numeric data were statistically evaluated by 1-way analysis of variance, followed by the Tukey–Kramer method for multiple comparisons. A P value less than 0.05 was considered to be statistically significant.

Results

Systolic blood pressure, heart rate, body weight, and heart weight/body weight ratio

The rats were subjected to Ang II infusion for 14 days, with or without administration of ANP. Compared with the controls (114 ± 5 mmHg), the Ang II and Ang II + ANP rats showed elevated SBP (Ang II, 204 ± 36 mmHg; Ang II + ANP, 201 ± 22 mmHg; $P < 0.001$). The Ang II rats had a significantly higher heart rate than the controls (control, 338 ± 12 beats/min; Ang II, 432 ± 53 beats/min; $P < 0.001$). In addition, the Ang II and Ang II + ANP rats had significantly lower body weights than the controls (control, 317 ± 18 g; Ang II, 216 ± 46 g; Ang II + ANP, 225 ± 45 g; $P < 0.001$). The Ang II rats had a significantly greater average heart weight/body weight ratio than the controls (control, 3.20 ± 0.55 mg/g; Ang II, 4.20 ± 1.02 mg/g; $P < 0.05$). The Ang II + ANP rats had a slightly, but not significantly, lower heart weight/body weight ratio compared with the Ang II rats (Ang II + ANP, 4.04 ± 0.78 mg/g; $P = 0.90$; Table 2). There were no significant differences between controls and ANP-alone rats in systolic blood pressure, heart rate, body weight, and heart weight/body weight ratio.

Ang II and Ang II + ANP rats showed comparable blood pressure and heart rate throughout the time course (Fig. 1).

Cardiac function

LVFS and EF were significantly lower in the Ang II rats than in the controls ($P < 0.001$), whereas the Ang II + ANP rats exhibited significantly higher LVFS and EF than the Ang II rats ($P < 0.001$). On the basis of Doppler spectra for

Table 2 Systolic blood pressure, heart rate, body weight, heart weight/body weight ratio, and echocardiographic parameters on day 14

	Control (n = 10)	Ang II (n = 10)	Ang II + ANP (n = 10)	ANP (n = 5)
Systolic blood pressure (mmHg)	114 ± 5	204 ± 36**	201 ± 22**	127 ± 5
Heart rate (beats/min)	338 ± 12	432 ± 53**	431 ± 76	352 ± 27
Body weight (g)	317 ± 18	216 ± 46**	225 ± 45**	306 ± 4
Heart weight/body weight (mg/g)	3.20 ± 0.55	4.20 ± 1.02*	4.04 ± 0.78	2.44 ± 0.11
LVDd (mm)	6.00 ± 0.35	4.14 ± 0.09**	4.36 ± 0.66	5.26 ± 1.20
LVDs (mm)	2.57 ± 0.37	2.12 ± 0.38*	1.83 ± 0.30	2.68 ± 0.77
EF (%)	92.1 ± 2.5	86.6 ± 2.5**	91.9 ± 2.1†	84.8 ± 8.8
FS (%)	57.9 ± 4.0	48.6 ± 3.1**	56.9 ± 4.1†	48.5 ± 10.3
E (cm/s)	0.78 ± 0.07	0.52 ± 0.08**	0.58 ± 0.09	0.61 ± 0.12
E/A	2.60 ± 0.27	1.98 ± 0.16**	2.13 ± 0.23	2.47 ± 0.41
DcT (ms)	67.4 ± 4.1	81.6 ± 5.5**	70.6 ± 3.0†	65.8 ± 4.8

Values are mean ± SD

LVDd left ventricular end-diastolic diameter, *LVDs* left ventricular end-systolic diameter, *EF* ejection fraction, *FS* fractional shortening, *E* peak velocity of mitral early inflow, *E/A* ratio of mitral early inflow peak velocity to atrial contraction-related flow peak velocity, *DcT* deceleration time

* $P < 0.05$ versus control, ** $P < 0.001$ versus control, † $P < 0.001$ versus Ang II

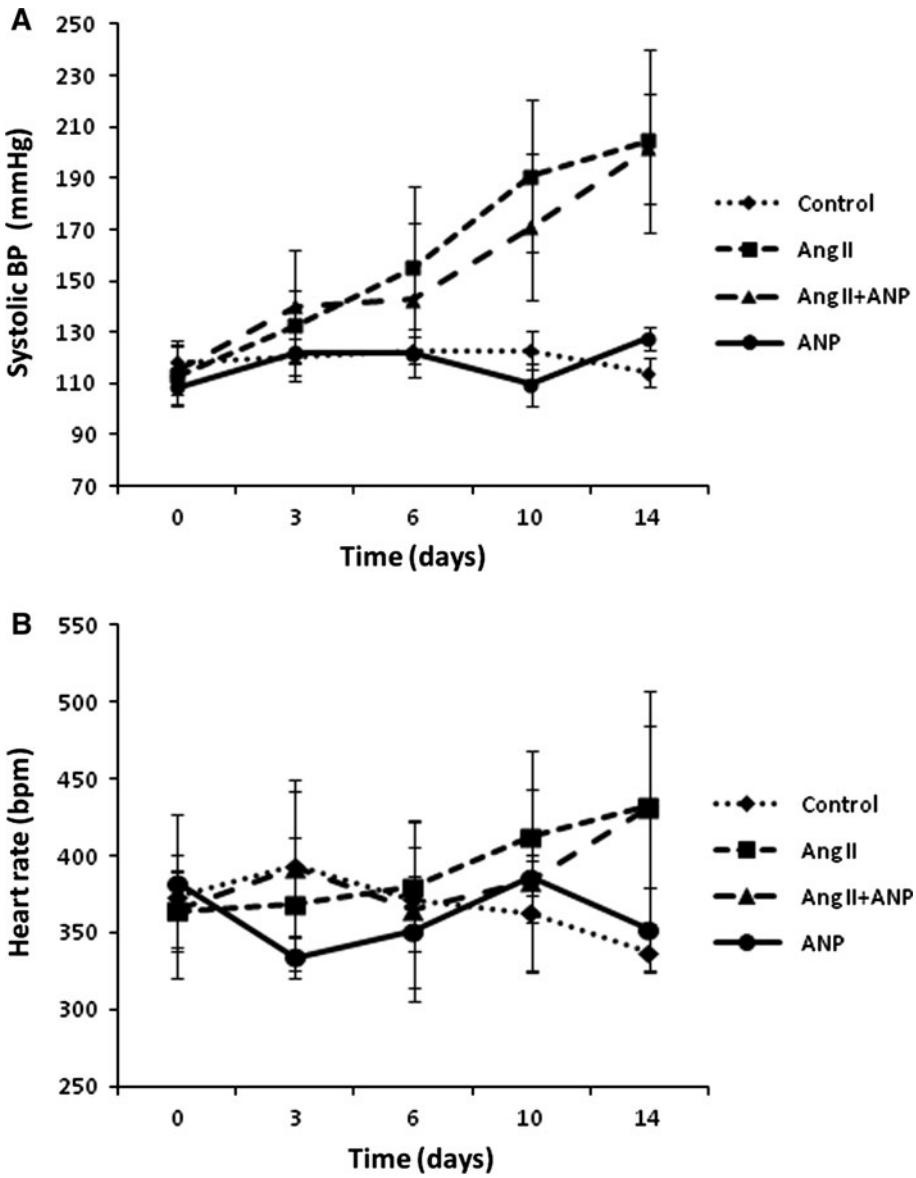

Fig. 1 The time course of systolic blood pressure (BP) (**a**) and heart rate (**b**). Values are expressed as mean ± SD. *Control* control rats, *Ang II* angiotensin II-treated rats, *Ang II + ANP* Ang II plus atrial natriuretic peptide-treated rats, *ANP* atrial natriuretic peptide-treated rats, *BPM* beats/min

transmitral flow, the Ang II rats showed significant decreases in *E* and *E/A* ratio, in addition to a significant prolongation of the DcT, compared with the controls (*E*, $P < 0.001$; *E/A*, $P < 0.001$; DcT, $P < 0.001$). Coadministration of ANP reversed the Ang II-mediated suppression of *E* and the *E/A* ratio, as well as the decreased DcT (*E*, $P = 0.22$; *E/A*, $P = 0.30$; DcT, $P < 0.001$; Table 2), indicating that ANP can partially reverse Ang II-induced ventricular dysfunction. There were no significant differences between controls and ANP-alone rats in echocardiographic parameters.

Myocyte hypertrophy

The average myocyte diameter was significantly greater in the Ang II rats than in the controls ($P < 0.001$). ANP coadministration significantly decreased myocyte diameter ($P < 0.01$; Fig. 2a, b). Compared with controls, the average myocyte diameter in ANP-alone rats showed no significant difference.

Myocardial fibrosis

The percent areas of myocardial fibrosis were significantly greater in the Ang II-treated rats than in the controls ($P < 0.001$). ANP coadministration significantly decreased interstitial fibrosis ($P < 0.01$; Fig. 3a, b). The mRNA levels of fibrotic indicators collagen type I (Fig. 3c) and collagen type III (Fig. 3d) were higher in the Ang II rats than in the controls, whereas ANP coadministration significantly decreased the mRNA levels of collagen type I (Fig. 3c) and collagen type III (Fig. 3d).

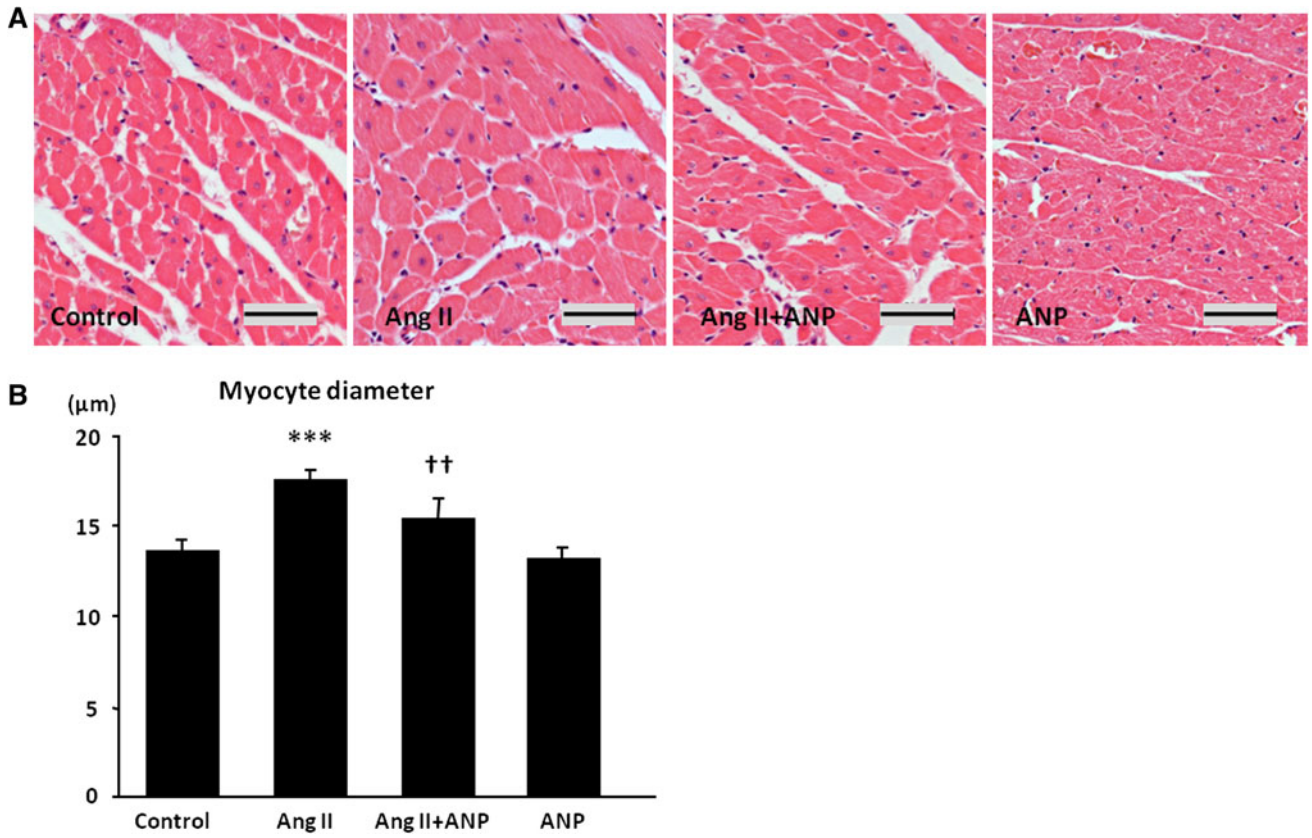

Fig. 2 Histological changes in the rat myocardium induced by chronic Ang II infusion. **a** Light micrographs of hematoxylin–eosin-stained sections (*scale bar* 50 μm). **b** The diameter of the myocytes. Values are expressed as mean ± SD. *Control* control rats, *Ang II* angiotensin II-treated rats, *Ang II + ANP* Ang II plus atrial natriuretic peptide-treated rats, *ANP* atrial natriuretic peptide-treated rats. ***$P < 0.001$ vs. the control group, $^{\dagger\dagger}P < 0.01$ vs. the Ang II group

Compared with controls, the percent areas of myocardial fibrosis in ANP-alone rats showed no significant difference. In addition, the mRNA levels of collagen type I and collagen type III of ANP-alone rats also showed no significant difference.

Cardiac inflammation

Immunostaining for TN-C is shown in Fig. 4a. The average TN-C-positive area was larger in the Ang II rats than in the controls, and again TN-C immunoreactivity was decreased by ANP coadministration. Similarly, the total number of CD68-positive cells per unit area (1 mm^2) was significantly greater in the Ang II rats than in the controls ($P < 0.001$; Fig. 4b, d). This increase was significantly decreased by ANP coadministration ($P < 0.05$; Fig. 4b, d). mRNA levels of TN-C (Fig. 4c) and MCP-1 (Fig. 4e) were increased in the Ang II rats compared with the controls, whereas ANP coadministration significantly decreased both TN-C (Fig. 4c) and MCP-1 (Fig. 4e) mRNA levels. Compared with controls, TN-C-positive area and the total number of CD68-positive cells in ANP-alone rats showed no significant difference. In addition, the mRNA levels of TN-C and MCP-1 of ANP-alone rats also showed no significant difference. The mRNA level of ET-1 was higher in the Ang II rats than in the controls. The mRNA level of ET-1 was decreased in the Ang II + ANP rats compared with the Ang II rats, but the difference was not statistically significant ($P = 0.38$, data not shown).

Confocal laser scanning microscopy

In the fibrotic area shown in Fig. 4a, b, by confocal laser scanning microscopy a large number of CD68-positive macrophages and α-SMA-positive cells, presumably myofibroblasts, was observed. We then compared whether TN-C immunopositivity colocalized with CD68 and α-SMA positivity. Most of the α-SMA-positive cells were found to be negative for TN-C staining (Fig. 5a), and CD68-positive macrophages were negative for TN-C staining (Fig. 5b).

Effects of ANP on TN-C synthesis by cardiac fibroblasts in culture

The effects of Ang II on TN-C and ET-1 gene expression, and the role of ET-1 receptors in Ang II- and ANP-mediated regulation of TN-C gene expression, were

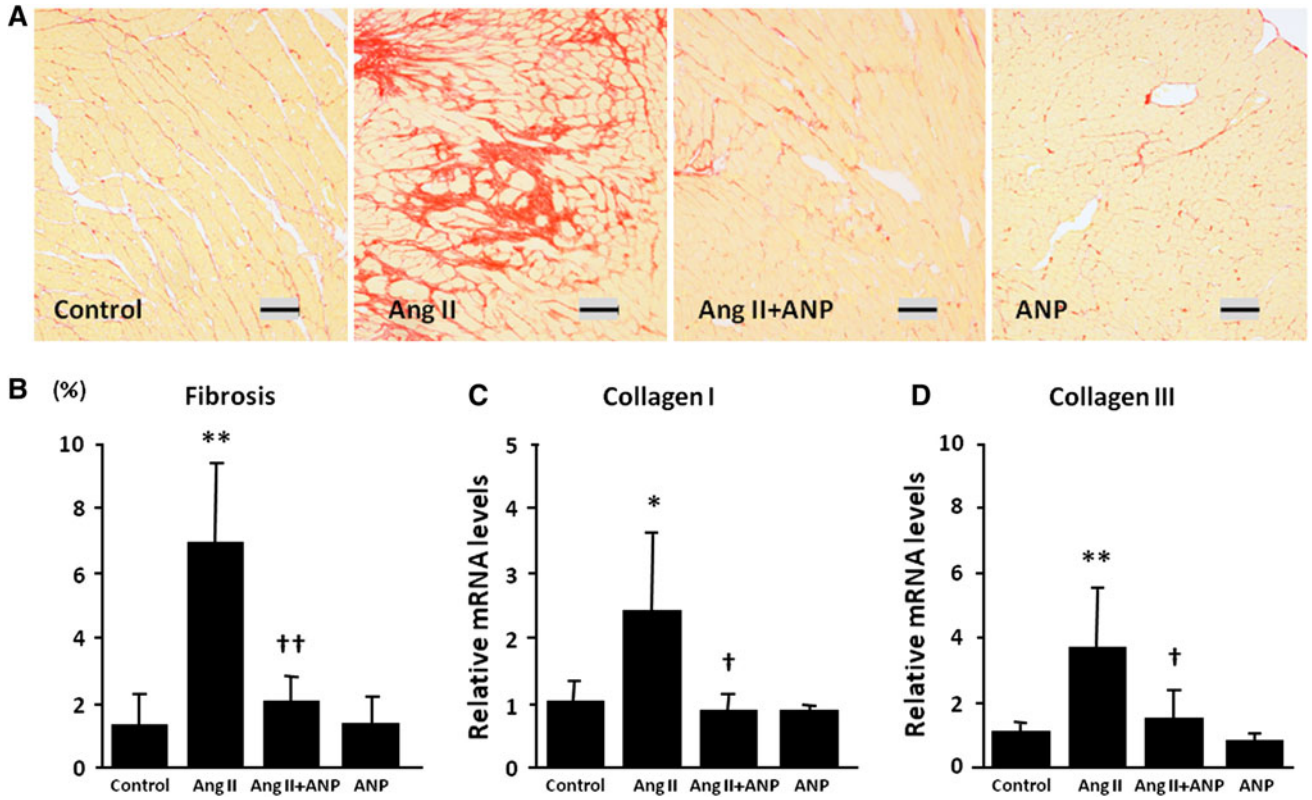

Fig. 3 Histological features of Ang II-induced myocardial fibrosis. **a** Light micrographs of Sirius Red staining (*scale bar* 100 μm). **b** Percent area of myocardial interstitial and perivascular fibrosis. **c** Relative mRNA levels of collagen I. **d** Relative mRNA levels of collagen III. Values are expressed as mean ± SD. *Control* control rats, *Ang II* angiotensin II-treated rats, *Ang II + ANP* Ang II plus atrial natriuretic peptide-treated rats, *ANP* atrial natriuretic peptide-treated rats. $^{*}P < 0.05$, $^{**}P < 0.01$ vs. the control group, $^{\dagger}P < 0.05$, $^{\dagger\dagger}P < 0.01$ vs. the Ang II group

examined in cultured cardiac fibroblasts by quantitative real-time RT-PCR. Ang II administration increased TN-C mRNA expression, and ANP coadministration significantly reversed this upregulation (Fig. 6a). In addition, Ang II increased ET-1 mRNA expression, whereas ANP coadministration significantly reversed this upregulation (Fig. 6b). Treatment of cultured cells with ET-1 significantly increased TN-C mRNA expression in a dose-dependent manner (Fig. 6c). Upregulation of Ang II-induced TN-C mRNA expression was significantly blocked by the ET-R antagonist bosentan and the ET-RA antagonist BQ123 (Fig. 6d, e), but not by the ET-RB antagonist BQ 788 (Fig. 6f).

Discussion

The present study clearly demonstrated that ANP treatment attenuates Ang II-induced cardiac inflammation, fibrosis, and hypertrophy, and improves systolic and/or diastolic cardiac function of the rat model.

It has been suggested that ANP may inhibit adverse cardiac remodeling by preventing cardiomyocyte hypertrophy and fibrosis based on G kinase activation [19, 35–37] in experiments using cultured cells and a natriuretic peptide receptor-deficient mice [38–40]. In our present study, ANP administration to rats significantly reversed Ang II-induced myocyte hypertrophy and fibrosis, which supports previous findings. Furthermore, we found that ANP obviously reduced infiltration of macrophages as well as expression of TN-C, an inflammatory marker, induced by Ang II administration.

The clinical significance of RAAS-mediated chronic myocardial inflammation is well recognized (reviewed in [41]). Inflammation and fibrosis are closely related; indeed, multiple factors associated with chronic inflammation are believed to induce fibrosis. Among these factors, matricellular proteins, a category of extracellular matrix molecules, have attracted considerable attention [31, 42]. Matricellular proteins do not contribute to the formation of fibers or basement membrane but rather serve as biological mediators by interacting directly with cells or regulating the activities of growth factors, cytokines, proteases, and other extracellular matrix proteins [43, 44]. TN-C is a typical matricellular protein expressed transiently at restricted sites during embryonic development, tissue

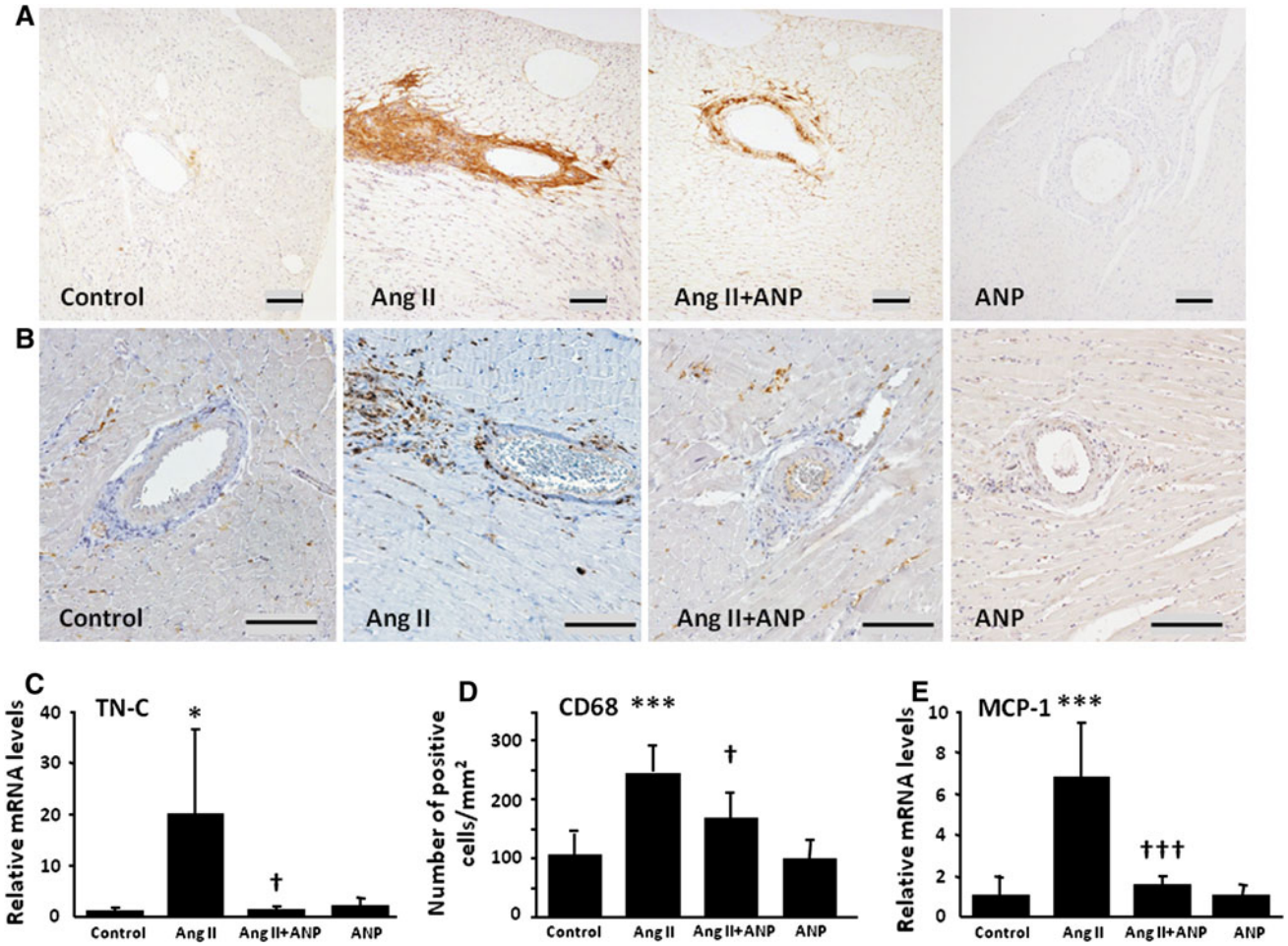

Fig. 4 **a** Changes in TN-C immunoreactivity in response to Ang II (*scale bar* 100 μm). **b** Immunostaining for CD68 (*scale bar* 100 μm). **c** Relative mRNA level of TN-C. **d** Total number of CD68-positive cells per unit area (1 mm^2). **e** Relative mRNA level of MCP-1. Values are expressed as mean ± SD. *Control* control rats, *Ang II* angiotensin II-treated rats, *Ang II + ANP* Ang II plus atrial natriuretic peptide-treated rats, *ANP* atrial natriuretic peptide-treated rats. $^{*}P < 0.05$, $^{***}P < 0.001$ vs. the control group, $^{\dagger}P < 0.05$, $^{\dagger\dagger\dagger}P < 0.001$ vs. the Ang II group

injury, inflammation, and fibrosis [45, 46]. Several lines of evidence suggest that TN-C could act as a profibrotic and proinflammatory modulator by enhancing macrophage activity [31, 47, 48]. In fact, deletion of the TN-C gene in mice attenuates hepatitis and liver fibrosis [49], rheumatoid arthritis [50], and fibrosis after myocardial infarction [51].

Several reports have suggested that ANP may have an anti-inflammatory effect [52, 53] and may inhibit macrophage activity [54]. We proposed that ANP may weaken inflammation by downregulation of TN-C, a modulator of inflammation.

In general, major sources of TN-C in myocardium could be the interstitial fibroblasts, as we have previously reported [25, 33]. Ang II upregulates TN-C expression in cultured cardiac fibroblasts as well as proinflammatory cytokines, growth factors, and reactive oxygen species [28]. We speculate that Ang II may stimulate interstitial fibroblasts to induce TN-C expression, which is reduced by ANP.

Using cultured cardiac fibroblasts, we found that ANP suppressed TN-C expression induced by Ang II. We investigated the role of ET-1 in Ang II/TN-C signaling because several recent studies have linked ET-1 to fibrosis, inflammation, and cardiovascular remodeling in the downstream signaling of Ang II [55]. Furthermore, it is well known that ANP suppresses gene expression of ET-1 of cardiac fibroblasts, as an autocrine/paracrine factor [56, 57], attributable to G kinase [56]. We first confirmed that Ang II upregulated ET-1 expression, which was suppressed by ANP, as reported previously [56]. Second, we examined if ET-1 is involved in TN-C upregulation by Ang II in fibroblasts. Dual ET-R and ET-RA blockade significantly suppressed TN-C upregulation, whereas ET-RB blockade did not. Conversely, ET-1 increased TN-C expression. Taken together, these in vitro results suggested that ANP may suppress Ang II-induced TN-C synthesis, at least in part, by inhibiting the ET-1/ET-RA signaling

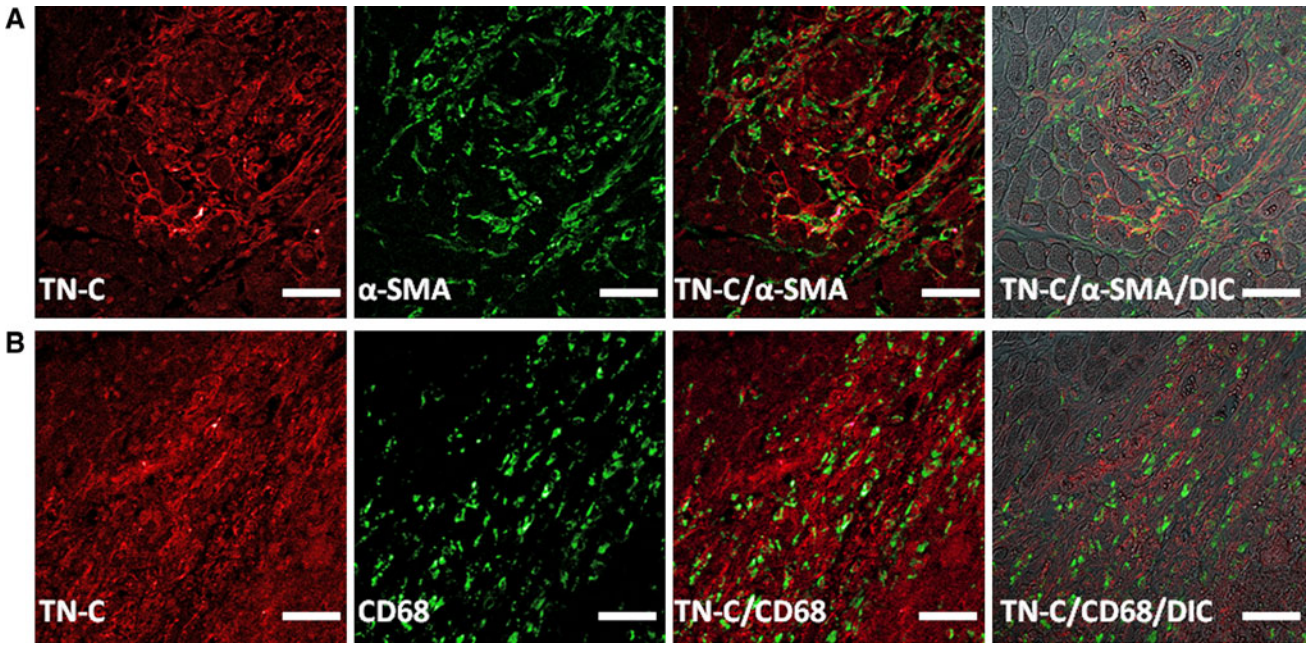

Fig. 5 Confocal laser scanning microscopy. Colocalization of tenascin-C (*TN-C*) with α-smooth muscle actin (*SMA*) (**a**) and CD68 (**b**) were examined. The *scale bar* indicates 50 μm. *DIC* Nomarski differential interference contrast imaging

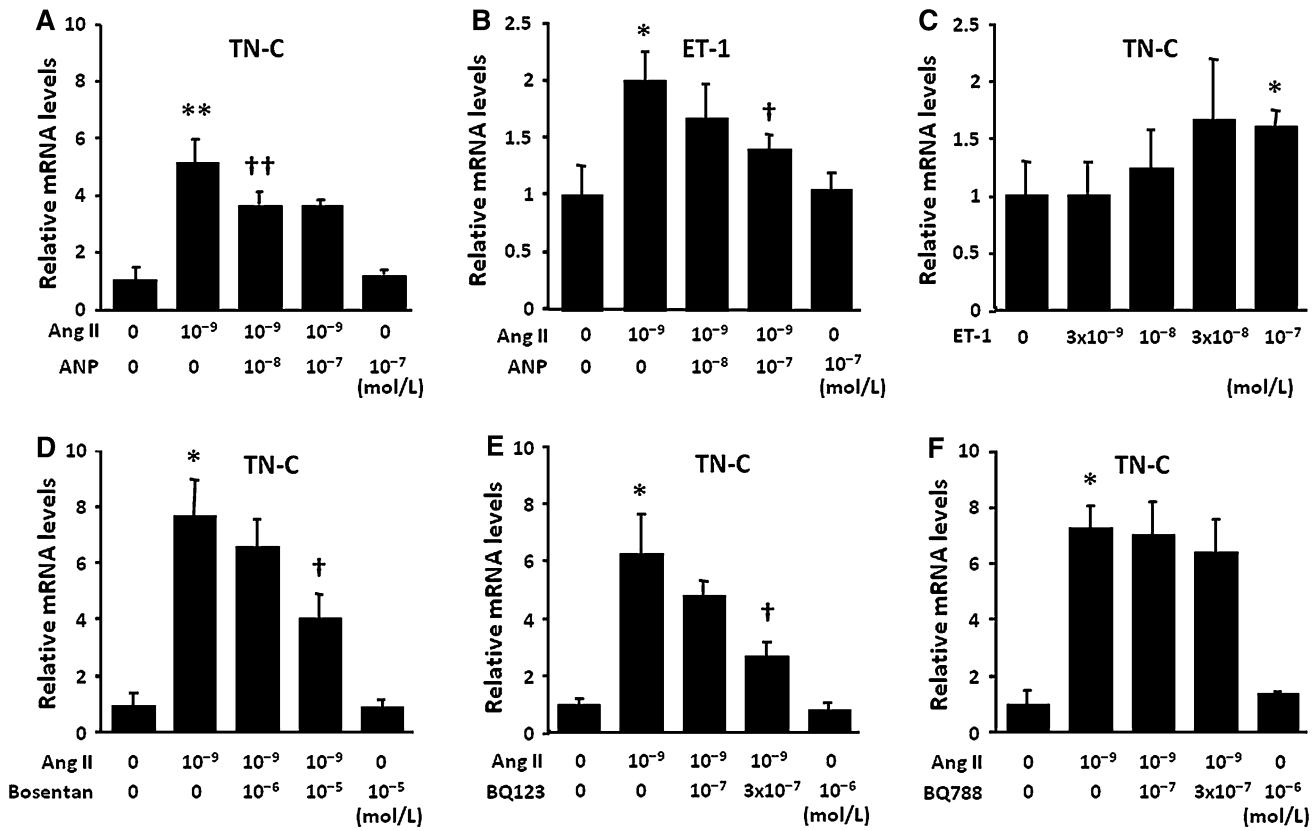

Fig. 6 ET-1 and TN-C synthesis by cardiac fibroblasts in culture. **a** Ang II increased the expression of TN-C mRNA, whereas ANP significantly decreased this upregulation. **b** Ang II increased the expression of ET-1 mRNA, which was significantly decreased by ANP. **c** ET-1 significantly increased TN-C mRNA expression in cardiac fibroblasts. Upregulation of Ang II-induced TN-C mRNA expression was significantly decreased by bosentan and BQ 123 (**d**, **e**), whereas BQ 788 had no significant effect (**f**). Values are expressed as mean ± SD. $^{*}P < 0.05$, $^{**}P < 0.01$ vs. no substance. $^{\dagger}P < 0.05$, $^{\dagger\dagger}P < 0.01$ vs. the Ang II alone group (10^{-9} mol/l)

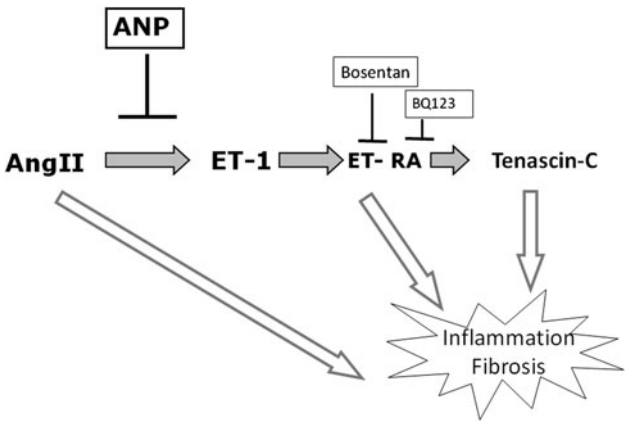

Fig. 7 A mechanism to explain how ANP attenuates inflammation and fibrosis of the myocardium. Ang II upregulates TN-C expression of cardiac fibroblasts, at least in part via ET-1/ET-RA, which may amplify inflammation and fibrosis. ANP suppresses Ang II-induced ET-1 expression, a possible enhancer of inflammation and fibrosis by itself, and in turn downregulates TN-C expression

pathway (Fig. 7). Recent reports have suggested that TN-C may enhance several signaling pathways, such as ET-1/ET-RA [58], transforming growth factor β [59], and platelet-derived growth factor [60] pathways. ANP may exert cardioprotective effects, at least partially, by suppressing TN-C that may modulate these inflammatory/fibrotic signaling cascades by creating a positive feedback loop (Fig. 7).

In the present study, we also clearly demonstrated that ANP treatment significantly attenuated cardiac hypertrophy without affecting blood pressure. As our group has previously reported, ANP can also suppress Ang II-induced cardiac hypertrophy by inhibiting the ET-1/ET-RA cascade [61, 62]. Therefore, ANP may exert a protective effect on cardiac interstitial cells as well as on cardiomyocytes, at least partly via the ET-1/ET-RA cascade.

Acknowledgments The authors thank M. Namikata for providing technical assistance, and also thank Dr Y. Ito (Division of Life Sciences, Department of Anatomy and Cell Biology, Osaka Medical College) for her excellent advice on confocal laser scanning microscopy, and A. Yamaki (ASUBIO Pharma Co., Ltd) for helpful discussion on the protocol design. This work was supported by JSPS Grants-in-Aid for Scientific Research #21590927(to K. I-Y.), and a research grant for intractable diseases from the Ministry of Health, Labor and Welfare of Japan (to K. I-Y. and Y. K.). Part of the study was also supported by a grant by Daiichi-Sankyo Co. Ltd.

References

1. Levin ER, Gardner DG, Samson WK (1998) Natriuretic peptides. N Engl J Med 339:321–328
2. Schultz HD, Gardner DG, Deschepper CF, Coleridge HM, Coleridge JC (1998) Vagal C-fiber blockade abolishes sympathetic inhibition by atrial natriuretic factor. Am J Physiol 255:R6–R13
3. Ehara S, Nakamura Y, Matsumoto K, Hasegawa T, Shimada K, Takagi M, Hanatani A, Izumi Y, Terashima M, Yoshiyama M (2012) Effects of intravenous atrial natriuretic peptide and nitroglycerin on coronary vasodilation and flow velocity determined using 3 T magnetic resonance imaging in patients with nonischemic heart failure. Heart Vessels. doi: 10.1007/s00380-012-0292-z
4. Kasamaki Y, Izumi Y, Ozawa Y, Ohta M, Tano A, Watanabe I, Hirayama A, Nakayama T, Kawamura H, Himit D, Mahemuti M, Sezai A (2012) Relationship between status of plasma atrial natriuretic peptide and heart rate variability in human subjects. Heart Vessels. doi:10.1007/s00380-012-0237-6
5. Kasama S, Furuya M, Toyama T, Ichikawa S, Kurabayashi M (2008) Effect of atrial natriuretic peptide on left ventricular remodeling in patients with acute myocardial infarction. Eur Heart J 29:1485–1494
6. Saito Y (2010) Roles of atrial natriuretic peptide and its therapeutic use. J Cardiol 56:262–270
7. Ishikawa C, Tsutamoto M, Wada A, Fujii M, Ohno K, Sakai H, Yamamoto T, Horie M (2005) Inhibition of aldosterone and endothelin-1 by carperitide was attenuated with more than 1 week of infusion in patients with congestive heart failure. J Cardiovasc Pharmacol 46:513–518
8. Tanaka T, Tsutamoto T, Sakai H, Nishiyama K, Fujii M, Yamamoto T, Horie M (2008) Effect of atrial natriuretic peptide on adiponectin in patients with heart failure. Eur J Heart Fail 10:360–366
9. Tsukamoto O, Fujita M, Kato M, Yamazaki S, Asano Y, Ogai A, Okazaki H, Asai M, Nagamachi Y, Maeda N, Shintani Y, Minamino T, Asakura M, Kishimoto I, Funahashi T, Tomoike H, Kitakaze M (2009) Natriuretic peptides enhance the production of adiponectin in human adipocytes and in patients with chronic heart failure. J Am Coll Cardiol 53:2070–2077
10. Hattori H, Minami Y, Mizuno M, Yumino D, Hoshi H, Arashi H, Nuki T, Sashida Y, Higashitani M, Serizawa N, Yamada N, Yamaguchi J, Mori F, Shiga T, Hagiwara N (2012) Differences in hemodynamic responses between intravenous carperitide and nicorandil in patients with acute heart failure syndromes. Heart Vessels. doi:1007/s00380-012-0252-7
11. Yamaji M, Tsutamoto T, Tanaka T, Kawahara C, Nishiyama K, Yamamoto T, Fujii M, Horie M (2009) Effect of carperitide on plasma adiponectin levels in acute decompensated heart failure patients with diabetes mellitus. Circ J 73:2264–2269
12. Nomura F, Kurobe N, Mori Y, Hikita A, Kawai M, Suwa M, Okutani Y (2008) Multicenter prospective investigation on efficacy and safety of carperitide as a first-line drug for acute heart failure syndrome with preserved blood pressure: COMPASS: carperitide effects observed through monitoring dyspnea in acute decompensated heart failure study. Circ J 72:1777–1786
13. Hata N, Seino Y, Tsutamoto T, Hiramitsu S, Kaneko N, Yoshikawa T, Yokoyama H, Tanaka K, Mizuno K, Nejima J, Kinoshita M (2008) Effects of carperitide on the long-term prognosis of patients with acute decompensated chronic heart failure: the PROTECT multicenter randomized controlled study. Circ J 72:1787–1793
14. Kuga H, Ogawa K, Oida A, Taguchi I, Nakatsugawa M, Hoshi T, Sugimura H, Abe S, Kaneko A (2003) Administration of atrial natriuretic peptide attenuates reperfusion phenomena and preserves left ventricular regional wall motion after direct coronary angioplasty for acute myocardial infarction. Circ J 67:443–448
15. Kasama S, Toyama T, Hatori T, Sumino H, Kumakura H, Takayama Y, Ichikawa S, Suzuki T, Kurabayashi M (2007) Effects of intravenous atrial natriuretic peptide on cardiac sympathetic nerve activity and left ventricular remodeling in patients

with first anterior acute myocardial infarction. J Am Coll Cardiol 49:667–674
16. Kitakaze M, Asakura M, Kim J, Shintani Y, Asanuma H, Hamasaki T, Seguchi O, Myoishi M, Minamino T, Ohara T, Nagai Y, Nanto S, Watanabe K, Fukuzawa S, Hirayama A, Nakamura N, Kimura K, Fujii K, Ishihara M, Saito Y, Tomoike H, Kitamura S; J-WIND investigators (2007) Human atrial natriuretic peptide and nicorandil as adjuncts to reperfusion treatment for acute myocardial infarction (J-WIND): two randomised trials. Lancet 370:1483–1493
17. Hayashi M, Tsutamoto T, Wada A, Maeda K, Mabuchi N, Tsutsui T, Horie M, Ohnishi M, Kinoshita M (2001) Intravenous atrial natriuretic peptide prevents left ventricular remodeling in patients with first anterior acute myocardial infarction. J Am Coll Cardiol 37:1820–1826
18. Tsuneyoshi H, Nishina T, Nomoto T, Kanemitsu H, Kawakami R, Unimonh O, Nishimura K, Komeda M (2004) Atrial natriuretic peptide helps prevent late remodeling after left ventricular aneurysm repair. Circulation 110:II174–II179
19. Tanaka K, Ito M, Kodama M, Hoyano M, Kimura S, Mitsuwa W, Hirono S, Adachi T, Watanabe K, Nakazawa M, Aizawa Y (2009) Long-term carperitide treatment attenuates left ventricular remodeling in rats with heart failure after autoimmune myocarditis. J Cardiovasc Pharmacol 54:232–239
20. Fiebeler A, Nussberger J, Shagdarsuren E, Rong S, Hilfenhaus G, Al-Saadi N, Dechend R, Wellner M, Meiners S, Maser-Gluth C, Jeng AY, Webb RL, Luft FC, Muller DN (2005) Aldosterone synthase inhibitor ameliorates angiotensin II-induced organ damage. Circulation 111:3087–3094
21. Kuwahara F, Kai H, Tokuda K, Takeya M, Takeshita A, Egashira K, Imaizumi T (2004) Hypertensive myocardial fibrosis and diastolic dysfunction: another model of inflammation? Hypertension 43:739–745
22. Rocha R, Rudolph AE, Frierdich GE, Nachowiak DA, Kekec BK, Blomme EA, McMahon EG, Delyani JA (2004) Aldosterone induces a vascular inflammatory phenotype in the rat heart. Am J Physiol 283:H1802–H1810
23. Endemann DH, Touyz RM, Iglarz M, Savoia C, Schiffrin EL (2004) Eplerenone prevents salt induced vascular remodeling and cardiac fibrosis in stroke-prone spontaneously hypertensive rats. Hypertension 43:1252–1257
24. Frangogiannis NG, Shimoni S, Chang SM, Ren G, Dewald O, Gersch C, Shan K, Aggeli C, Reardon M, Letsou GV, Espada R, Ramchandani M, Entman ML, Zoghbi WA (2002) Active interstitial remodeling: an important process in the hibernating human myocardium. J Am Coll Cardiol 39:1468–1474
25. Imanaka-Yoshida K, Hiroe M, Yasutomi Y, Toyozaki T, Tsuchiya T, Noda N, Maki T, Nishikawa T, Sakakura T, Yoshida T (2002) Tenascin-C is a useful marker for disease activity in myocarditis. J Pathol 197:388–394
26. Imanaka-Yoshida K, Matsumoto K, Hara M, Sakakura T, Yoshida T (2003) The dynamic expression of tenascin-C and tenascin-X during early heart development in the mouse. Differentiation 71:291–298
27. Morimoto S, Imanaka-Yoshida K, Hiramitsu S, Kato S, Ohtsuki M, Uemura A, Kato Y, Nishikawa T, Toyozaki T, Hishida H, Yoshida T, Hiroe M (2005) Diagnostic utility of tenascin-C for evaluation of the activity of human acute myocarditis. J Pathol 205:460–467
28. Nishioka T, Suzuki M, Onishi K, Takakura N, Inada H, Yoshida T, Hiroe M, Imanaka-Yoshida K (2007) Eplerenone attenuates myocardial fibrosis in the angiotensin II-induced hypertensive mouse: involvement of tenascin-C induced by aldosterone-mediated inflammation. J Cardiovasc Pharmacol 49:261–268
29. Tamura A, Kusachi S, Nogami K, Yamanishi A, Kajikawa Y, Hirohata S, Tsuji T (1996) Tenascin expression in endomyocardial biopsy specimens in patients with dilated cardiomyopathy: distribution along margin of fibrotic lesions. Heart 75:291–294
30. Tsukada B, Terasaki F, Shimomura H, Otsuka K, Otsuka K, Katashima T, Fujita S, Imanaka-Yoshida K, Yoshida T, Hiroe M, Kitaura Y (2009) High prevalence of chronic myocarditis in dilated cardiomyopathy referred for left ventriculoplasty: expression of tenascin-C as a possible marker for inflammation. Human Pathol 40:1015–1022
31. Okamoto H, Imanaka-Yoshida K (2012) Matricellular proteins: new molecular targets to prevent heart failure. Cardiovasc Ther 30:198–209
32. Imanaka-Yoshida K (2012) Tenascin-C in cardiovascular tissue remodeling. From development to inflammation and repair. Circ J 76:2513–2520
33. Imanaka-Yoshida K, Hiroe M, Nishikawa T, Ishiyama S, Shimojo T, Ohta Y, Sakakura T, Yoshida T (2001) Tenascin-C modulates adhesion of cardiomyocytes to extracellular matrix during tissue remodeling after myocardial infarction. Lab Invest 81:1015–1024
34. Tamaoki M, Imanaka-Yoshida K, Yokoyama K, Nishioka T, Inada H, Hiroe M, Sakakura T, Yoshida T (2005) Tenascin-C regulates recruitment of myofibroblasts during tissue repair after myocardial injury. Am J Pathol 167:71–80
35. Calderone A, Thaik CM, Takahashi N, Chang DL, Colucci WS (1998) Nitric oxide, atrial natriuretic peptide, and cyclic GMP inhibit the growth-promoting effects of norepinephrine in cardiac myocytes and fibroblasts. J Clin Invest 101:812–818
36. Hayashi D, Kudoh S, Shiojima I, Zou Y, Harada K, Shimoyama M, Imai Y, Monzen K, Yamazaki T, Yazaki Y, Nagai R, Komuro I (2004) Atrial natriuretic peptide inhibits cardiomyocyte hypertrophy through mitogen-activated protein kinase phosphatase-1. Biochem Biophys Res Commun 322:310–319
37. Holtwick R, van Eickels M, Skryabin BV, Baba HA, Bubikat A, Begrow F, Schneider MD, Garbers DL, Kuhn M (2003) Pressure-independent cardiac hypertrophy in mice with cardiomyocyte-restricted inactivation of the atrial natriuretic peptide receptor guanylyl cyclase-A. J Clin Invest 111:1399–1407
38. Oliver PM, Fox JE, Kim R, Rockman HA, Kim HS, Reddick RL, Pandey KN, Milgram SL, Smithies O, Maeda N (1997) Hypertension, cardiac hypertrophy, and sudden death in mice lacking natriuretic peptide receptor A. Proc Natl Acad Sci USA 94:14730–14735
39. Knowles JW, Esposito G, Mao L, Hagaman JR, Fox JE, Smithies O, Rockman HA, Maeda N (2001) Pressure-independent enhancement of cardiac hypertrophy in natriuretic peptide receptor A-deficient mice. J Clin Invest 107:975–984
40. Kishimoto I, Rossi K, Garbers DL (2001) A genetic model provides evidence that the receptor for atrial natriuretic peptide (guanylyl cyclase-A) inhibits cardiac ventricular myocyte hypertrophy. Proc Natl Acad Sci USA 98:2703–2706
41. Manabe I (2011) Chronic inflammation links cardiovascular, metabolic and renal diseases. Circ J 75:2739–2748
42. Dobaczewski M, Gonzalez-Quesada C, Frangogiannis NG (2010) The extracellular matrix as a modulator of the inflammatory and reparative response following myocardial infarction. J Mol Cell Cardiol 48:504–511
43. Bornstein P (1995) Diversity of function is inherent in matricellular proteins: an appraisal of thrombospondin 1. J Cell Biol 130:503–506
44. Bornstein P, Sage EH (2002) Matricellular proteins: extracellular modulators of cell function. Curr Opin Cell Biol 14:608–616
45. Midwood KS, Hussenet T, Langlois B, Orend G (2011) Advances in tenascin-C biology. Cell Mol Life Sci 68:3175–3199
46. Chiquet-Ehrismann R, Tucker RP (2011) Tenascins and the importance of adhesion modulation. Cold Spring Harb Perspect Biol 3

47. Kanayama M, Morimoto J, Matsui Y, Ikesue M, Danzaki K, Kurotaki D, Ito K, Yoshida T, Uede T (2011) α9β1 integrin-mediated signaling serves as an intrinsic regulator of pathogenic Th17 cell generation. J Immunol 187:5851–5864
48. Udalova IA, Ruhmann M, Thomson SJ, Midwood KS (2011) Expression and immune function of tenascin-C. Crit Rev Immunol 31:115–145
49. El-Karef A, Yoshida T, Gabazza EC, Nishioka T, Inada H, Sakakura T, Imanaka-Yoshida K (2007) Deficiency of tenascin-C attenuates liver fibrosis in immune-mediated chronic hepatitis in mice. J Pathol 211:86–94
50. Midwood K, Sacre S, Piccinini AM, Inglis J, Trebaul A, Chan E, Drexler S, Sofat N, Kashiwagi M, Orend G, Brennan F, Foxwell B (2009) Tenascin-C is an endogenous activator of Toll-like receptor 4 that is essential for maintaining inflammation in arthritic joint disease. Nat Med 15:774–780
51. Nishioka T, Onishi K, Shimojo N, Nagano Y, Matsusaka H, Ikeuchi M, Ide T, Tsutsui H, Hiroe M, Yoshida T, Imanaka-Yoshida K (2010) Tenascin-C may aggravate left ventricular remodeling and function after myocardial infarction in mice. Am J Physiol Heart Circ Physiol 298:H1072–H1078
52. Moriyama N, Taniguchi M, Miyano K, Miyoshi M, Watanabe T (2006) ANP inhibits LPS-induced stimulation of rat microglial cells by suppressing NF-kappaB and AP-1 activations. Biochem Biophys Res Commun 350:322–328
53. Ladetzki-Baehs K, Keller M, Kiemer AK, Koch E, Zahler S, Wendel A, Vollmar AM (2007) Atrial natriuretic peptide, a regulator of nuclear factor-kappa B activation in vivo. Endocrinology 148:332–336
54. Kiemer AK, Hartung T, Vollmar AM (2000) cGMP-mediated inhibition of TNF-alpha production by the atrial natriuretic peptide in murine macrophages. J Immunol 165:175–181
55. Leask A (2010) Potential therapeutic targets for cardiac fibrosis: TGFbeta, angiotensin, endothelin, CCN2, and PDGF, partners in fibroblast activation. Circ Res 106:1675–1680
56. Fujisaki H, Ito H, Hirata Y, Tanaka M, Hata M, Lin M, Adachi S, Akimoto H, Marumo F, Hiroe M (1995) Natriuretic peptides inhibit angiotensin II-induced proliferation of rat cardiac fibroblasts by blocking endothelin-1 gene expression. J Clin Invest 96:1059–1065
57. Glenn DJ, Rahmutula D, Nishimito M, Liang F, Gardner DG (2009) Atrial natriuretic peptide suppresses endothelin gene expression and proliferation in cardiac fibroblasts through a GATA4-dependent mechanism. Cardiovasc Res 84:209–217
58. Lange K, Kammerer M, Hegi ME, Grotegut S, Dittmann A, Huang W, Fluri E, Yip GW, Gotte M, Ruiz C, Orend G (2007) Endothelin receptor type B counteracts tenascin-C-induced endothelin receptor type A-dependent focal adhesion and actin stress fiber disorganization. Cancer Res 67:6163–6173
59. Nagaharu K, Zhang X, Yoshida T, Katoh D, Hanamura N, Kozuka Y, Ogawa T, Shiraishi T, Imanaka-Yoshida K (2011) Tenascin C induces epithelial-mesenchymal transition-like change accompanied by SRC activation and focal adhesion kinase phosphorylation in human breast cancer cells. Am J Pathol 178:754–763
60. Ishigaki T, Imanaka-Yoshida K, Shimojo N, Matsushima S, Taki W, Yoshida T (2011) Tenascin-C enhances crosstalk signaling of integrin αvβ3/PDGFR-β complex by SRC recruitment promoting PDGF-induced proliferation and migration in smooth muscle cells. J Cell Physiol 226:2617–2624
61. Ito H, Hirata Y, Hiroe M, Tsujino M, Adachi S, Takamoto T, Nitta M, Taniguchi K, Marumo F (1991) Endothelin-1 induces hypertrophy with enhanced expression of muscle-specific genes in cultured neonatal rat cardiomyocytes. Circ Res 69:209–215
62. Ito H, Hirata Y, Adachi S, Tanaka M, Tsujino M, Koike A, Nogami A, Marumo F, Hiroe M (1993) Endothelin-1 is an autocrine/paracrine factor in the mechanism of angiotensin II-induced hypertrophy in cultured rat cardiomyocytes. J Clin Invest 92:398–403